PAPER

In-plane oriented highly ordered lamellar structure formation of poly(N-dodecylacrylamide) induced by humid annealing†

Yuki Hashimoto,[a] Takuma Sato,[a] Ryosuke Goto,[b] Yuki Nagao,[c] Masaya Mitsuishi,[d] Shusaku Nagano[b] and Jun Matsui*[e]

In this paper, we report that poly(N-dodecylacrylamide) (pDDA) formed a well-ordered lamellar structure by annealing in humid conditions. Differential scanning calorimetry measurements of pDDA showed that the crystallized part of the dodecyl side chain in nanodomains melted at −28.5 °C and a glass transition temperature of 73.6 °C, indicating that pDDA is an amorphous polymer at room temperature (20 °C). Thin films of pDDA were prepared by spin coating. Two-dimensional grazing-angle incidence X-ray diffraction (GI-XRD) measurements indicated that the film is composed of randomly oriented lamellar domains. When the film was annealed under 98% relative humidity at 60 °C for 24 h, the GI-XRD imaging plate showed spot-like diffraction in the out-of-plane direction with second-order and third-order peaks, indicating that the lamellar plane is oriented parallel to the substrate plane. The lamellar spacing was determined to be 3.25 nm from the Bragg peak. Fourier transform infrared measurements of lamellar structured films showed that the dodecyl side chains are aligned perpendicular to the lamellar plane.

Introduction

Microphase-separated block copolymers have attracted much attention because of their unique structure as well as their application to several fields, such as nanostructure templates,[1–4] solar cells,[5] and ion-conductive membranes.[6–8] Highly ordered structures, such as lamellae, spheres, and gyroids, with periodic sizes of a few tens to hundreds of nanometers have been formed by microphase separation of chemically different blocks. In contrast, Beiner *et al.* reported that a homopolymer with long alkyl side chains formed a nanophase segregated structure.[9–11] In the nanosegregated structure, the alkyl chains aggregated, forming nanodomains with sizes of 0.5–2.0 nm. Nanophase separation occurred because of the incompatibility between the

alkyl side chains and the main chains. The segregated structure formation mechanism is similar to that observed in the lyotropic liquid crystal. Several polymers such as poly(n-alkyl acrylates),[10,11] poly(n-alkyl methacrylates),[10,11] and poly(alkyl thiophenes)[12,13] form the nanophase separated structure. The nanodomain structures are strongly dependent on the alkyl side chain length and are independent of the main chain chemical composition. However, the nanodomains are randomly oriented, and uniformly oriented lamellae are not present in amorphous alkyl side chain polymers.[10,11]

Several long alkyl side chain polymers have been reported to form a monolayer at the air–water interface.[14–16] For example, poly(N-dodecylacrylamide) (pDDA) (Fig. 1) forms a stable monolayer at the air–water interface because of the strong hydrogen-bonding network between amide groups.[17,18] Moreover, the monolayer can be transferred onto a solid substrate using the Langmuir–Blodgett (LB) technique. Recently, we reported a high proton-conductive film using a poly(N-
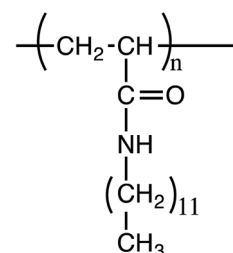
[a]Graduate School of Science and Engineering, Yamagata University, 1-4-12 Kojirakawa-machi, Yamagata 990-8560, Japan

[b]Department of Molecular Design and Engineering, Graduate School of Engineering, Nagoya University, Furo-cho, Chikusa, Nagoya 464-8603, Japan

[c]School of Materials Science, Japan Advanced Institute of Science and Technology, 1-1 Asahidai, Nomi, Ishikawa 923-1292, Japan

[d]Institute for Multidisciplinary Research for Advanced Materials, Tohoku University, 2-1-1 Katahira, Aoba-ku, Sendai 980-8577, Japan

[e]Department of Material and Biological Chemistry, Yamagata University, 1-4-12 Kojirakawa-machi, Yamagata 990-8560, Japan. E-mail: jun_m@sci.kj.yamagata-u.ac.jp

Fig. 1 Chemical structure of pDDA.

dodecylacrylamide-*co*-acrylic acid) LB film.[19] The high proton conduction in the copolymer LB film can be attributed to formation of a two-dimensional (2D) proton-conductive nano-channel in the interlayer of the LB film by humid annealing. Therefore, it is important to investigate the effect of humidity on the nanostructure of pDDA to understand the proton-conduction mechanism in the thin film.

In this study, we prepared a uniformly oriented lamellar film of pDDA by annealing a spin coted film in humid conditions. The lamellar structure was evaluated by X-ray diffraction (XRD), grazing-angle incidence XRD (GI-XRD), and Fourier transform infrared (FT-IR) spectroscopy.

Experimental section

N-Dodecylacrylamide (DDA) was synthesized by reacting *N*-dodecylamine with acryloyl chloride in the presence of triethylamine. pDDA was prepared using free radical polymerization of DDA with 2,2′-azobis(isobutyronitrile) as a thermal initiator in toluene. The number average molecular weight (M_n) and polydispersity index (M_w/M_n) were determined to be 22 000 and 2.7, respectively, using a gel permeation chromatograph (Tosoh Corp.) with a polystyrene standard. Hydrophilic silicon substrates were prepared by treatment with a UV-O$_3$ cleaner (UV253; SEN Lights Corp.). Hydrophobic silicon substrates were prepared by immersing the cleaned substrate in a *ca.* 1 × 10^{-6} M octyltrichlorosilane (Shinetsu Chemical Co.) chloroform solution. Thermogravimetric analysis (TGA) was performed in air at a heating rate of 10 °C min^{-1} (TGA-50H; Shimadzu Corp.). The transition temperatures of dry and water-adsorbed pDDA were measured using a differential scanning calorimeter (DSC-2C; PerkinElmer Inc., Norwalk, CT) under nitrogen flow (20 ml min^{-1}) with a heating rate of 20 °C min^{-1}. To measure the glass transition temperature (T_g) of water-adsorbed pDDA under humid conditions, about 6 mg of pDDA powder was place in an aluminum pan and the powder was incubated at 60 °C and 98% relative humidity (RH) for 24 h. The pan was then rapidly sealed for the measurement.

FT-IR spectra were recorded on a Jasco FT/IR 4200 FT-IR spectrometer (Jasco Corp.). Incident-angle-dependent FT-IR spectra were recorded on a Nicolet 6700 FT-IR spectrometer (Nicolet) equipped with a mercury cadmium telluride detector (Thermo Fischer Scientific Inc.). The p-polarized infrared (IR) probe light incidence was set normal to the substrate and the incident angle (α) was varied from 0° (normal) to 38° by rotating the sample (Fig. 5c). Single-beam spectra were collected by changing α. 2D GI-XRD measurements were performed using a Rigaku FR-E X-ray diffractometer with an R-AXIS IV 2D detector (Rigaku Corp., Japan). We used Cu Kα radiation (λ = 0.1542 nm) with a beam size of approximately 300 μm × 300 μm. The camera length was 300 mm. The sample stage was composed of a goniometer and a vertical stage (ATS-C316-EM/ALV-300-HM; Chuo Precision Industrial Co. Ltd.). The incidence angle was chosen as 0.18–0.22°. One-dimensional (1D) XRD measurements were performed on a Rigaku Smartlab diffractometer (Rigaku Corporation) with a Cu Kα X-ray source (λ = 0.1542 nm) using a scintillation counter as the detector.

The measurements were carried out by the symmetrical reflection geometry (θ–2θ) method. The thickness of the pDDA film was measured by stylus profilometry (DektakXT; Bruker). The water uptake dynamics of the pDDA film was investigated using a quartz crystal microbalance (QCM) (THQ-100P-SW; Tamadevice Co., Ltd, Japan) equipped with a flow cell. The humidity and temperature in the cell were controlled by a humidity controller (Bel Flow-1; BEL Japan, Inc., Japan) and a cool incubator (ICI1 1-6112-01; As-One, Japan). Polished 9 MHz crystals (Tamadevice Co., Ltd) were used for the measurements. The temperature and humidity in the cell were monitored with a data logger (RTR-507; T&D Corporation).

Results and discussion

The thermal properties of pDDA were investigated by TGA and DSC measurements. pDDA starts to decompose at 190 °C (Fig. S1†). The DSC third heating curves of pristine pDDA and water-adsorbed pDDA are shown in Fig. 2. The DSC thermogram of pristine pDDA shows two characteristic transitions. The first transition, with a peak at −28.5 °C, is attributed to the melting temperature (T_M) of the crystallized part of the dodecyl side chain in the nanodomains.[20] The temperature is similar to that reported by Beiner *et al.* for poly(*n*-dodecyl methacrylate).[20] The broad endothermic peak indicates that a small number (∼6%) of the alkyl carbon atoms in the dodecyl chains are crystallized.[20] The second transition at 73.6 °C is assigned to the glass transition temperature of pDDA. The glass transition temperature of the water-adsorbed pDDA decreased to 56.4 °C because water can weaken the hydrogen-bonded network in the acrylamide backbones and act as a plasticizer. The results show that pDDA is in the fully amorphous polymer state at room temperature. A thin film of pDDA was prepared by spin coating pDDA toluene solution (5 wt%) onto a hydrophobic silicon substrate. The film was vacuum dried at 80 °C for 1 h to evaporate the solvent. The film thickness was determined to be approximately 470 nm using a surface profiler. 2D GI-XRD measurements of the spin-coated film show a broad scattering hemicycle at q_y = 2.3 nm^{-1} (d = 2.7 nm) (Fig. 3a). The d value is attributed to the layer spacing of the lamellae in the nanodomains. The d value is comparable with the values for poly(*n*-dodecyl acrylate) and poly(*n*-dodecyl methacrylate) films.[11] The isotropic hemicycle pattern reflects the randomly oriented lamellar nanodomains in the dry annealed film. As previously reported by Beiner *et al.*, the alkyl side chains are interdigitated
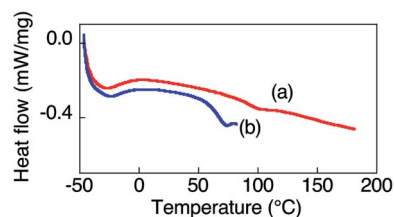

Fig. 2 DSC thermograms of (a) pristine pDDA and (b) water-adsorbed p(DDA).
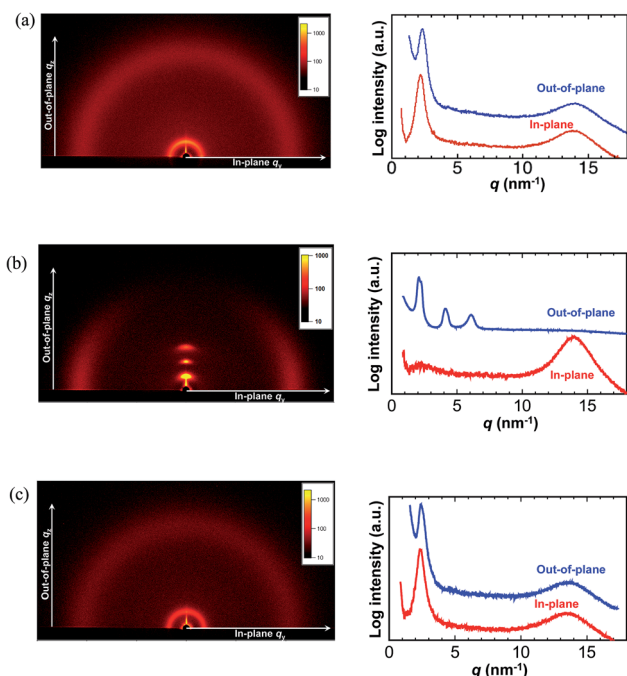
Fig. 3 2D XRD data of pDDA films under different annealing conditions: (a) as-cast, (b) annealed at 60 °C and RH 98% for 24 h, and (c) post-annealed at 60 °C under dry conditions for 12 h. In each part, the left-hand and right-hand figures show the 2D-XRD pattern and 1D intensity profile (red, in-plane (q_y) direction; blue, out-of-plane (q_z) direction), respectively. The 1D intensity profiles were extracted from the 2D images.

in the lamellar nanodomains. The film was successively placed in a humidity and temperature-controlled chamber, and annealed at 98% RH and 60 °C for 24 h. Fig. 3b shows the 2D scattering image of the film annealed in humid conditions. The strong spot-like diffractions exhibit a spot at $q_z = 2.1$ nm^{-1} in the out-of-plane direction with higher order peaks ($q_z = 4.1$ and 6.1 nm^{-1}). The 2D XRD pattern shows that the highly ordered lamellar structure formed parallel to the substrate plane. Moreover, in-plane scattering with a vertical arc is observed around $q_y = 14$ nm^{-1}. The 1D profile in the in-plane direction shows a wide halo, which indicates that the dodecyl side chains are in an amorphous state (Fig. 3b, right).[21,22] The results agree with the DSC measurements, which indicate that the alkyl side chains are in a "molten state" at room temperature (20 °C). The layer spacing of the highly oriented lamellar structure is larger than that of the lamellae in the nanodomains because the alkyl side chains have a non-interdigitated alignment in the highly oriented lamellae, which is discussed in the following section. The 2D GI-XRD pattern of the lamellar structured film post-annealed at 60 °C in dry conditions for 12 h shows a pattern resembling that of the initial film (Fig. 3c), which indicates that the uniformly planer-oriented lamellar structure returned to the initial disordered lamellar phase. Furthermore, the film can be converted back to the uniformly planer-oriented lamellae by annealing the film in humid conditions, which indicates that humidity is extremely important to initiate formation of the highly ordered oriented lamellar structure in the pDDA system.

The q_z value is not quite accurate in a GI-XRD measurement due to the underestimate from the incident angle and out of the Ewald sphere condition. In order to obtain an accurate value of the highly ordered lamellar spacing, we performed out-of-plane 1D XRD measurements of the annealed film using the θ–2θ method. Diffraction peaks of the lamellar structure are observed at $q = 1.93$, 3.90, and 5.82 nm^{-1} (Fig. 4a). The ratio of the diffraction peaks is $1 : 2 : 3$, which strongly supports lamellae formation. The lamellar spacing was determined to be 3.25 nm from the diffraction pattern, and the spacing is attributed to the length of two dodecyl side chains (Fig. 4b). The planar ordering of the lamellae increased with increasing annealing time and temperature. In the case of the film annealed for 1 h under the same conditions, only the first-order Bragg peak at $q = 2.05$ nm^{-1} is observed with a scattering intensity of about ~1400 cps (Fig. 4c and S2†). There is no trace of the higher order peaks. With increasing annealing time, the intensity increases and the lamella peak shifts to the lower q region. Therefore, the lamellar spacing increased. The full width at half maximum (FWHM) of the first peak is 0.167 nm^{-1} for 1 h annealing. With increasing annealing time, the FWHM gradually decreases and becomes almost constant for annealing times longer than 24 h (Fig. 4d). Moreover, higher order scattering peaks emerge for longer annealing time (Fig. S2†). A similar trend is observed with temperature. Higher temperature results in smaller q and a narrower first-order peak with second- and third-order peaks (Fig. S3†). Usually, long-range lamellar ordering in comb-like polymers is ascribed to crystallization of the long alkyl side chains.[9,23] However, from the GI-XRD results, the dodecyl side chains in the in-plane oriented pDDA lamellar film are in an amorphous state. Therefore, the formation mechanism of the highly ordered in-plane oriented lamellar
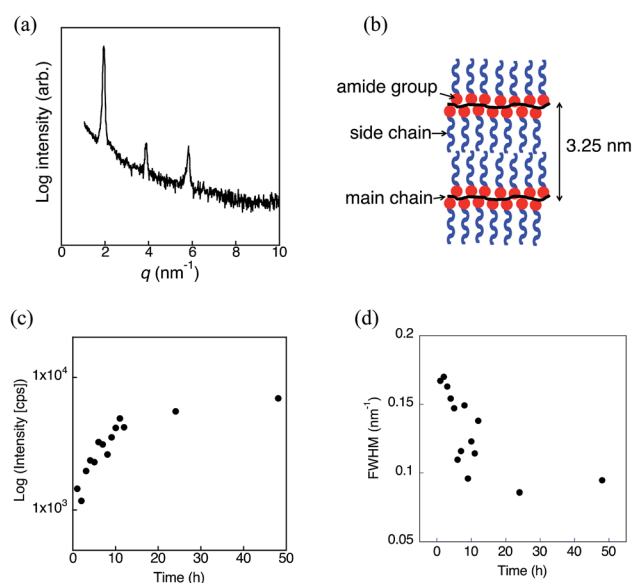

Fig. 4 (a) Out-of-plane XRD pattern of the pDDA film annealed at 60 °C and 98% RH for 24 h obtained by the θ–2θ method. (b) Schematic representation of the highly ordered lamellar structure of pDDA. (c) Scattering intensity and (d) FWHM values of the first peak at different annealing times.

pDDA film greatly differs from that in semicrystalline comb-like polymers. The lamellar structure also formed on a hydrophilic silicon substrate, which indicates that the surface properties of the substrate do not affect structure formation (Fig. S4†).

The lamellar structure was further investigated by FT-IR spectroscopy (Fig. 5a and S5†). Based on the XRD results, the pDDA film annealed at 24 h under 98% RH at 60 °C was used for the FT-IR measurements. The IR absorption peak wavenumbers of the CH_2 groups before and after annealing in humid conditions were compared to discuss the conformation of the dodecyl side chains. It has been reported that the absorption bands related to the asymmetric (ν_a) and symmetric (ν_s) CH_2 stretching modes are sensitive to the conformation of the hydrocarbon. When the side chains are in the all-*trans* zigzag conformation, the peaks appear at 2918 ± 1 cm^{-1} (ν_a) and 2848 ± 1 cm^{-1} (ν_s), respectively. The peaks shift to longer wavelengths of 2927 ± 1 cm^{-1} (ν_a) and 2856 ± 1 cm^{-1} (ν_s) in the fully disordered conformation.[24,25] The as-cast pDDA film has absorption peaks at $\nu_a = 2924$ cm^{-1} and $\nu_s = 2854$ cm^{-1}. These peaks shifted to lower wavenumbers ($\nu_a = 2922$ cm^{-1} and $\nu_s = 2852$ cm^{-1}) after humid annealing, which indicates that the number of *trans* conformers of the CH_2 groups increased in the lamellar film (Fig. 5b). A negative wavenumber shift has been observed in the *trans*-rich form of pDDA for a highly oriented ordered LB film.[26] Therefore, it can be concluded that the dodecyl side chains have a *trans*-rich conformation. Furthermore, the amide I peaks are sensitive to the hydrogen bonding conformation.[27] The amide I peak is located at 1642 cm^{-1} for the lamellar structured film. The peak regions show that the amide bond has an α-helix or random-coil structure with a random hydrogen-bonded network.[27] Although it is difficult to ascertain which structure is formed, the random hydrogen-bonded structure could be dominant in the planar lamellar structure.

To obtain further insight into the uniformly planer-oriented lamellar structure, the alkyl side chain orientation was investigated by incident-angle-dependent IR absorption of CH_2. If the long alkyl chains have an all *trans* structure, the maximum absorption of CH_2 stretching is obtained when the incident angle of the IR probe light matches the tilt angle of the dodecyl side chains (Fig. 5c).[26,28] This phenomenon occurs because the CH_2 stretching transition moment is perpendicular to the long axis of the alkyl chain. As previously mentioned, the dodecyl side chains are in a *trans*-rich conformation. Therefore, incident-angle-dependent IR absorption can be used to estimate the orientation of the dodecyl side chains. It is noteworthy that the number of effective molecules for IR absorption varies with the incident angle to the film. This effect was corrected by measuring angle-dependent IR spectra of the nonoriented polystyrene film and preparing a calibration curve. Fig. 5d shows the angle-dependent absorption of CH_2 asymmetric stretching of the lamellar structured film. The absorbance increases with decreasing incident angle and reaches a maximum at $\alpha = 8°$. This indicates that the alkyl side chains are almost perpendicularly aligned with respect to the substrate. It has been reported that the molecular length of the dodecyl side chain is 1.80 nm when it takes the all-*trans* conformation.[26] Therefore, the lamellar spacing was calculated to be 3.58 nm when the dodecyl side chains are tilted at 8° and not interdigitated. The lamellar spacing was determined to be 3.25 nm from the out-of-plane XRD measurement. Compared with the calculated value, the actual value is 0.33 nm shorter. This suggests that not all of the dodecyl side chains have an all-*trans* conformation and the gauche conformer is present in the lamellar structure.

The response of the pDDA film to humidity change was investigated by QCM measurements. QCM was unstable at 60 °C under high humidity condition, therefore the measurements were carried out at 25 °C (Fig. S6†). The amount of water absorbed in the pDDA film increases with increasing RH and about 15 wt% of water adsorbed at the film at 98% RH (Fig. S6a†). The response to the RH change is rapid and it almost follows the RH change dynamics (Fig. S6b†). Before the measurements, all of the samples were dried (20 °C and 30% RH) for a few hours. Therefore, absorbed water amount is at most ∼3 wt% (Fig. S6a†). These results suggest that the uniformly oriented lamellae are retained even if water desorbs. Hence, the probable mechanism for the highly ordered lamellar structure by humid annealing is as follows. During annealing in humid conditions, water mainly absorbs in the hydrophilic amide main chain region, which increases the hydrophilic volume in the polymer film. The hydrophobic and hydrophilic volumes then become similar, which favors lamellae formation.[29] As revealed by DSC measurements, T_g decreased in the water-adsorbed pDDA therefore the polymer chains are mobile in the annealed condition. The hydrophilic amide region of the polymer segregates to the surface because the air–polymer interface is highly hydrophilic in high humidity conditions. This surface segregation results in the dodecyl side chains orientating perpendicular to the substrate. The oriented dodecyl side chains act as the starting region for lamellae formation. The lamellar structure is stable in the room temperature even the water is desorbed because the T_g is higher than room temperature.
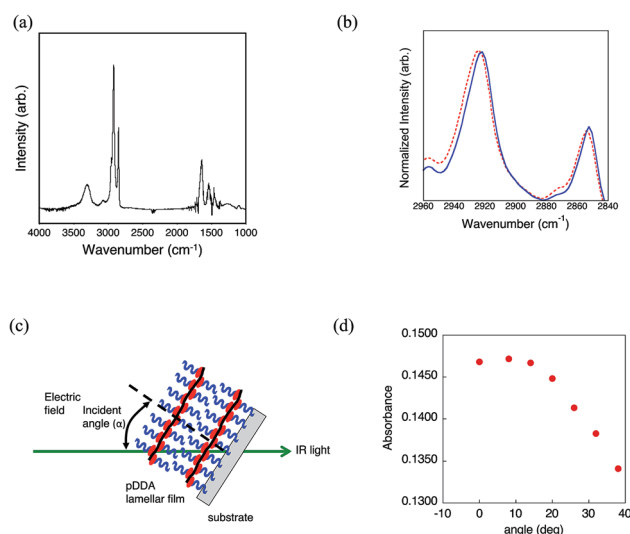

Fig. 5 (a) FT-IR spectra of the pDDA film after annealing at 60 °C and 98% RH. (b) FT-IR spectra of the CH_2 stretching region of the pDDA film before (dotted red line) and after annealing (solid blue line) at 60 °C and 98% RH for 24 h. (c) Configuration of the incident angle and lamellar structured pDDA film. (d) IR absorbance at 2922 cm^{-1} with different angles of incident.

Conclusion

Amorphous pDDA films formed a uniformly oriented lamellar structure by annealing in humid conditions. The lamellar plane was aligned parallel to the substrate with the dodecyl side chains aligned perpendicular to the lamellar plane. The alkyl side chains remained amorphous in the lamellar structured film. It is proposed that the change of the volume ratio and χ parameter between the hydrophilic and hydrophobic regions by humid annealing is the driving force for uniformly planer-oriented lamellae formation. To elucidate the proposed mechanism, the effects of the alkyl side chain length and hydrophilic groups on lamellae formation are currently being investigated. Similar highly oriented lamellar films have been prepared by side chain liquid crystal polymers.[22] Moreover, a block copolymer of the liquid crystal (LC) polymer with poly ethylene glycol (PEO) form a film with uniform straight molecular channels of PEO units, which was applied as an ion conductive channels.[30–32] Our present results proposed the simple strategy to prepare a highly oriented polymer lamella structure without particular thermotropic LC structures. The oriented lamellar film was constructed from a simple amorphous pDDA with a flexible side chain by annealing in humid conditions. Furthermore, the lamellar structure is stable in water condition. These results indicate that chemical and physical properties of pDDA lamellar film are close to biomembranes. Recently, we have reported that the two-dimensional proton nanochannel constructed in the interlayer of pDDA nanosheet assembly shows a fast proton conduction.[19] A similar two-dimensional nanochannel can be simply prepared by the present process, which suggests the lamellar film has a potential for high proton conductive membranes. Applications of the highly oriented lamellar film to ion transfer materials are now in progress.

Acknowledgements

References

1 H. G. Yoo, M. Byun, C. K. Jeong and K. J. Lee, *Adv. Mater.*, 2015, **27**, 3982–3998.

2 H.-C. Kim, S.-M. Park and W. D. Hinsberg, *Chem. Rev.*, 2010, **110**, 146–177.

3 R. G. Hobbs, N. Petkov and J. D. Holmes, *Chem. Mater.*, 2012, **24**, 1975–1991.

4 *Directed Self-assembly of Block Co-polymers for Nano-manufacturing*, ed. R. Gronheid and P. Nealey, Elsevier, Cambridge, 2015.

5 K. Nakabayashi and H. Mori, *Materials*, 2014, **7**, 3274–3290.

6 K. Miyatake, B. Bae and M. Watanabe, *Polym. Chem.*, 2011, **2**, 1919.

7 O. Diat and G. Gehel, in *Block Copolymers in Nanoscience*, ed. M. Lazzari, G. Liu and S. Lecommandoux, John Wiley & Sons, 2007, ch. 15, pp. 337–367.

8 G. He, Z. Li, J. Zhao, S. Wang, H. Wu, M. D. Guiver and Z. Jiang, *Adv. Mater.*, 2015, **27**, 5280–5295.

9 E. Hempel, H. Budde, S. Höring and M. Beiner, *J. Non-Cryst. Solids*, 2006, **352**, 5013–5020.

10 S. Hiller, O. Pascui, H. Budde, O. Kabisch, D. Reichert and M. Beiner, *New J. Phys.*, 2004, **6**, 10.

11 M. Beiner and H. Huth, *Nat. Mater.*, 2003, **2**, 595–599.

12 S. Pankaj, E. Hempel and M. Beiner, *Macromolecules*, 2009, **42**, 716–724.

13 S. Pankaj and M. Beiner, *J. Phys. Chem. B*, 2010, **114**, 15459–15465.

14 J. Kumaki, *Polym. J.*, 2016, **48**, 3–14.

15 I. I. I. D. H. McCullough and S. L. Regen, *Chem. Commun.*, 2004, 2787–2791, DOI: 10.1039/b410027c.

16 K. Ariga, Y. Yamauchi, T. Mori and J. P. Hill, *Adv. Mater.*, 2013, **25**, 6477–6512.

17 M. Mitsuishi, J. Matsui and T. Miyashita, *Polym. J.*, 2006, **38**, 877–896.

18 M. Mitsuishi, J. Matsui and T. Miyashita, *J. Mater. Chem.*, 2009, **19**, 325–329.

19 T. Sato, Y. Hayasaka, M. Mitsuishi, T. Miyashita, S. Nagano and J. Matsui, *Langmuir*, 2015, **31**, 5174–5180.

20 E. Hempel, H. Huth and M. Beiner, *Thermochim. Acta*, 2003, **403**, 105–114.

21 A. K. Chatterjee, S. D. Phatak, P. S. Murthy and G. C. Joshi, *J. Appl. Polym. Sci.*, 1994, **52**, 887–894.

22 N. A. Platé and V. P. Shibaev, *Comb-Shaped Polymers and Liquid Crystals*, Springer, US, 1987.

23 N. A. Kuznetsov, V. M. Moiseyenko, Z. A. Roganova, A. L. Smolyanskii and V. P. Shibayev, *Vysokomol. Soedin., Ser. A*, 1977, **19**, 399–408.

24 Z. Zhang, A. L. Verma, M. Yoneyama, K. Nakashima, K. Iriyama and Y. Ozaki, *Langmuir*, 1997, **13**, 4422–4427.

25 J. Umemura, D. G. Cameron and H. H. Mantsch, *Biochim. Biophys. Acta, Biomembr.*, 1980, **602**, 32–44.

26 Y. Mizuta, M. Matsuda and T. Miyashita, *Langmuir*, 1993, **9**, 1158–1159.

27 Y. Nagao, J. Matsui, T. Abe, H. Hiramatsu, H. Yamamoto, T. Miyashita, N. Sata and H. Yugami, *Langmuir*, 2013, **29**, 6798–6804.

28 H. Nakahara and K. Fukuda, *J. Colloid Interface Sci.*, 1979, **69**, 24–33.

29 J. N. Israelachvili, *Intermolecular and Surface Forces*, Academic Press, New York, 2nd edn, 1992.

30 L. Wen, K. Xiao, A. V. Sainath, M. Komura, X. Y. Kong, G. Xie, Z. Zhang, Y. Tian, T. Iyoda and L. Jiang, *Adv. Mater.*, 2016, **28**, 757–763.

31 P. W. Majewski, M. Gopinadhan, W.-S. Jang, J. L. Lutkenhaus and C. O. Osuji, *J. Am. Chem. Soc.*, 2010, **132**, 17516–17522.

32 J. Li, K. Kamata, M. Komura, T. Yamada, H. Yoshida and T. Iyoda, *Macromolecules*, 2007, **40**, 8125–8128.